# SCIENTIFIC REP🅞RTS

**OPEN**

# Role of P2X₄ Receptor in Mouse Voiding Function

Weiqun Yu, Warren G. Hill, Simon C. Robson & Mark L. Zeidel

Purinergic signalling plays an important role in the regulation of bladder smooth muscle (BSM) contractility, and P2X₄ receptor is expressed in the bladder wall, where it may act by forming heteromeric receptors with P2X₁, the major purinergic force-generating muscle receptor. To test this hypothesis, we examined mouse BSM contractile properties in the absence and presence of selective P2X₁ (NF449 & NF279) and P2X₄ antagonists (5-BDBD). These drugs inhibited BSM purinergic contraction only partially, suggesting the possibility of a heteromeric receptor. However, carefully controlled co-immunoprecipitation experiments indicated that P2X₁ and P2X₄ do not form physically linked heteromers. Furthermore, immunofluorescence staining showed that P2X₄ is not present in mouse BSM *per se*, but in an unknown cellular structure among BSM bundles. To investigate whether deletion of P2X₄ could impact voiding function *in vivo*, P2X₄ null mice were characterized. P2X₄ null mice had normal bladder weight and morphology, normal voiding spot size and number by voiding spot assay, normal voiding interval, pressure and compliance by cystometrogram, and normal BSM contractility by myography. In conclusion, these data strongly suggest that P2X₄ is not present in mouse BSM cells, does not affect smooth muscle contractility and that mice null for P2X₄ exhibit normal voiding function.

The prevalence of lower urinary tract symptoms (LUTS) is extremely high, affecting ~50% of the population aged more than 40 years old[1,2], and the major symptoms of LUTS are manifested by bladder contraction (voiding) and relaxation (storage) disorders. Mechanistic understanding of LUTS is still unclear, however, purinergic signalling is a major pathway in modulating bladder physiology/pathophysiology. In normal human bladders, atropine blocks ~95% of nerve-mediated bladder smooth muscle (BSM) contraction (induced by electrical field stimulation-EFS), leading many to conclude that purinergic contractility is insignificant. However, a deeper look at the literature reveals controversy and unresolved questions: the neuromuscular purinergic component in female bladders and in the bladder trigone accounts for about 50% and 40% of nerve-mediated contraction force respectively[3,4]. Furthermore, externally applied α,β-meATP (as opposed to EFS-stimulated neuronal release) elicited significant human BSM contraction, and purinegic receptors like P2X₁ is highly expressed in human bladder[5,6]. In human bladder with pathological conditions, contraction in response to neuromuscular purinergic signalling can account for up to 65% of total force in patients with overactive bladder, partial bladder outlet obstruction, and diabetic bladder dysfunction (DBD)[7–12], and elevated ATP release/altered P2X receptor expression have been reported in these patients. The importance of purinergic signalling in regulating bladder function is further supported by recent findings from two human patients with ectonucleotidase ENTPD1 mutation, who display bladder hypomotility and incontinence, in addition to neurological conditions[13].

Current evidence on purinergic component or atropine-resistant contractile force in BSM contraction favours a dominant role for P2X₁. First, P2X₁ receptor is the major purinergic receptor expressed in BSM. Second, BSM from P2X₁ deficient mice lose the majority of their purinergic force, which is perhaps unsurprising since P2X₁ is believed to initiate the rapid contraction phase in BSM[14]. However, there is additional important evidence that purinergic receptors other than P2X₁ play an important role. First, RT-PCR or immunoblotting studies reveal that multiple P2X receptors are expressed in bladder[15–18]. Second, in guinea pig bladder, significant neurogenic contractions can be elicited even in the presence of cholinergic and P2X₁ receptor antagonists[19]. Third, in diabetic rat models like streptozotocin (STZ) treatment or Zucker obese rats, bladders exhibited significant non-cholinergic and non-α,β-meATP sensitive contractions accounting for 20% of total nerve mediated contractile force[20,21]. These results suggest that there are additional P2 receptors active in BSM and indeed abundant expression of P2X₄ has been observed by immunostaining in BSM as well as in other smooth muscle[22]. Since P2X receptors

Department of Medicine, Beth Israel Deaconess Medical Center and Harvard Medical School, Boston, Massachuesetts, USA. Correspondence and requests for materials should be addressed to W.Y. (email: wyu2@bidmc.harvard.edu)
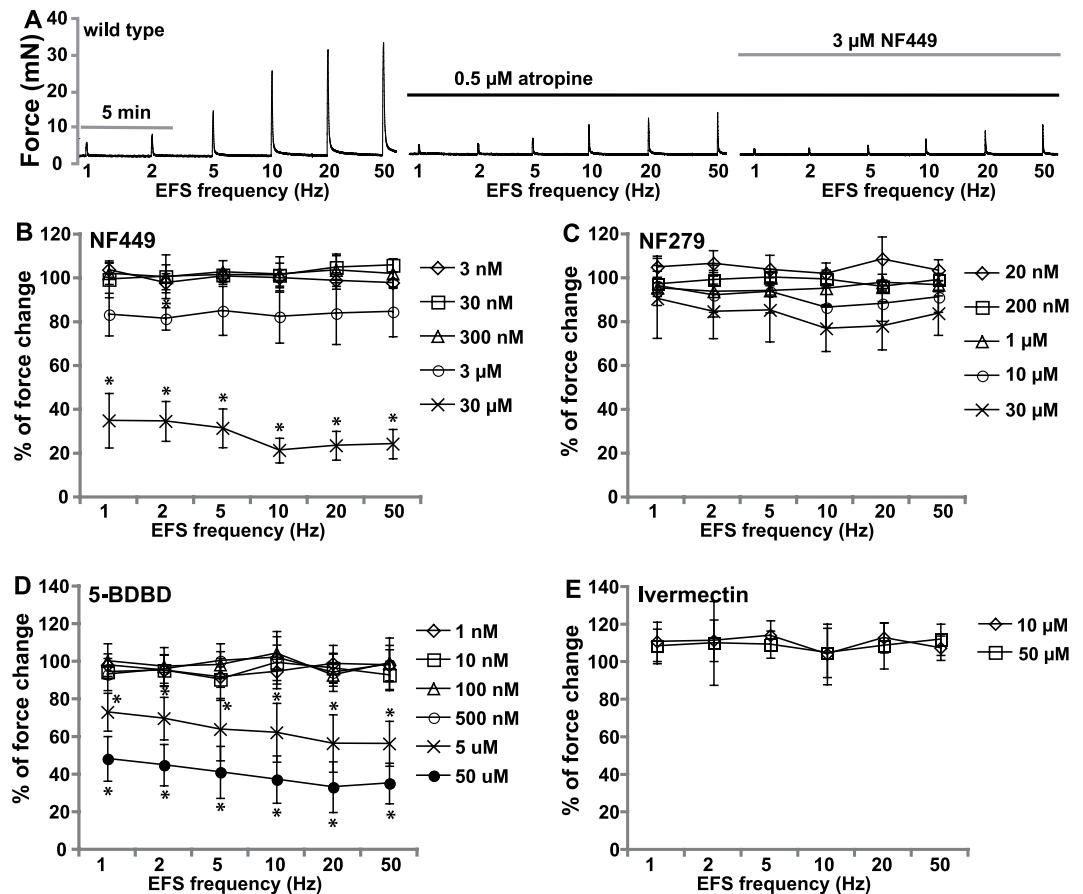
**Figure 1.** Pharmacological properties of BSM contractility. BSM strips were stimulated by EFS at indicated frequencies in increasing order ((**A**)-left). Raw data showing effect of sequential addition of atropine and NF449 (pre-treatment 15 min) on EFS force ((**A**)-right panels). Selective P2X$_1$ antagonists NF449 ((**B**), n = 7), NF279 ((**C**), n = 4), or selective P2X$_4$ antagonist 5-BDBD ((**D**), n = 7), or P2X$_4$ potentiator, Ivermectin ((**E**), n = 8) were then added at indicated concentrations (with accumulative addition) for 15 min to measure the atropine-resistant force change in BSM contraction in response to EFS. Force changes were normalized to control and shown as percentages. These data indicate that P2X$_1$ and P2X$_4$ antagonists only partially inhibit BSM atropine resistant force at relatively high concentrations. Ivermectin, a P2X$_4$ potentiator, does not increase BSM atropine resistant force significantly. BSM atropine resistant force before drug treatment was used as control (100%), and drug effect (inhibition or potentiation) was normalized to control. Data were analysed using one-way ANOVA and then Bonferroni's multiple comparison post-hoc tests. * indicates $P < 0.05$ when compared to control.

are trimeric and in many tissues, heteromeric (with mixed P2 subtypes), this raises the question of whether P2X$_4$ forms either functional homomers or possibly functional heterotrimers with P2X$_1$ and thereby participates in BSM contraction[23].

To determine the potential role of P2X$_4$ in BSM function, we have examined BSM contraction in the absence and presence of P2X$_4$ antagonists. We have also used co-immunoprecipitation techniques to examine whether P2X$_4$ forms heteromers with P2X$_1$. Finally we have determined the role of P2X$_4$ in overall voiding function by studying a P2X$_4$ knockout mouse.

## Results

### Pharmacological characterization does not support a P2X$_1$ homomer in BSM.
During electric field stimulation (EFS), BSM contraction is stimulated through cholinergic and non-cholinergic (or purinergic) neurotransmitter release. In the presence of atropine, cholinergic stimulation is eliminated, permitting assay of atropine resistant or purinergic contraction. P2X$_1$ is sensitive to α,β-meATP, but many other P2X receptors, including some P2X heteromers are also sensitive to α,β-meATP[24–26]. Potent and more selective P2X$_1$ antagonists such as NF449 (IC50 = 0.28 nM) and NF279 (IC50 = 19 nM) are now well documented[24]. We therefore examined the ability of these antagonists to alter the contraction force developed by BSM strips, in response to EFS in the presence of sufficient atropine to block the cholinergic response. As shown in Fig. 1, these P2X$_1$ antagonists were only marginally effective in attenuating EFS-induced, atropine-resistant contractions (Fig. 1B,C). NF449 did inhibit BSM contraction significantly at a concentration of 30 μM, a level 10$^5$ times higher than the IC$_{50}$, at which selectivity is lost and the antagonist inhibits most P2X subunits (Fig. 1B). NF279 did not show any significant inhibition on BSM contraction even when the concentration reached 30 μM (Fig. 1C). P2X$_4$ is a unique P2X
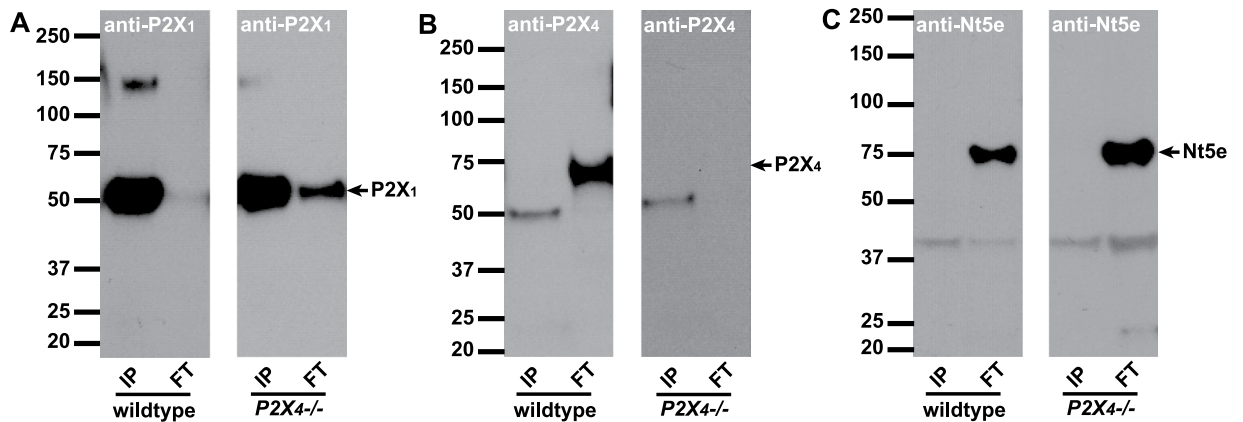
**Figure 2.** Immunoprecipitation with anti-P2X$_1$ antibody. Antibodies to P2X$_1$ were immobilized onto resin beads and then incubated with mouse bladder lysates to IP the antigen and co-IP interacting proteins. Proteins that were bound (IP: 2.5 μg protein/lane) or did not bind (FT: 25 μg protein/lane) to the beads were resolved by SDS-PAGE, and Western blots were probed with A) P2X$_1$, B) P2X$_4$ or C) Nt5e antibodies. (**A**) Left and right panels show P2X$_1$ immunoblots on IP and FT lysates from wild type and *P2X$_4$*−/− mice. Monomeric P2X$_1$ can be seen highly concentrated in the pulldown fraction at 50 kDa. Little P2X$_1$ appears in FT. (**B**) P2X$_4$ antibody detects P2X$_4$ as a band at 70 kDa in wild type, but is completely absent in *P2X$_4$*−/− mice. The antibody shows minor cross-reactivity to possibly P2X$_1$. Note, there is no evidence of the 70 kDa band in the IP lane. (**C**) An antibody to 5′-nucleotidase (Nt5e) demonstrates that pulldown with anti-P2X$_1$ is 'clean' with no non-specific protein binding evident in the IP lanes.

receptor which does not show sensitivity to most P2X agonists and antagonists[24]. 5-BDBD (IC50 = 0.5 μM) might be the most potent P2X$_4$ antagonist available. We showed that it was able to inhibit EFS induced atropine-resistant BSM contractions at concentrations between 0.5–50 μM (Fig. 1D), indicating that P2X$_4$ might be involved in BSM contraction. By contrast, ivermectin (EC$_{50}$ = 0.2 μM), a large macrocyclic lactone that is known to potentiate P2X$_4$ channel current did not increase EFS-induced atropine-resistant BSM contraction at concentrations as high as 50 μM (Fig. 1E). In summary, there were weak effects using the specific antagonists alone, suggesting that BSM might contain a pharmacologically unique heteromeric P2X$_1$ trimer, and that P2X$_4$ could participate as a subunit of the trimer.

**P2X$_1$ and P2X$_4$ heteromers were not detectable by immunoprecipitation.** To test the hypothesis suggested by the pharmacology, we attempted to co-immunoprecipitate both proteins. The specificity of the anti-P2X$_1$ antibody we used, has been validated previously on bladder tissues from a knockout mouse[27,28], and our results demonstrate that a specific protein band at around 50 kD becomes highly enriched when bladder protein lysate is immunoprecipitated with it (Fig. 2A). This was true for bladders from wild type as well as P2X4 null mice. In the right panel of Fig. 2A we see evidence of a small amount of unbound P2X1 in the flow-through (FT) fraction. No protein is immunoprecipitated when the antibody is omitted from the pull-down (data not shown), indicating that detected protein is specifically bound to the antibody.

We performed immunoprecipitation with the anti-P2X$_1$ antibody to examine whether P2X$_4$ protein could be co-immunoprecipitated along with P2X$_1$ (Fig. 2B). The anti-P2X$_4$ antibody has also been validated previously for its specificity, using knockout mice[29]. P2X$_4$ protein (~70 kD) was only detected in the non-bound FT samples of wild type mice (Fig. 2B, left panel). There was no ~70 kD band in the IP lane. Strikingly, the positive identification of P2X$_4$ in the flow through was confirmed by its absence in P2X$_4$ knockout samples (Fig. 2B, right panel). There was in addition a band at detected ~50 kD by P2X$_4$ antibody. Since it appears in the co-IP'd lanes of both wild type and *P2X$_4$*−/− tissue and is the same molecular size as P2X$_1$, there is a very strong likelihood that the P2X$_4$ antibody shows minor cross-reactivity to P2X$_1$.

As a further control for the specificity of the co-IP we blotted P2X$_1$ pulldown samples with anti-Nt5e antibody, an enzyme that converts AMP to adenosine and which we have identified in BSM previously[30] (Fig. 2C). The results showed that Nt5e protein was only present in non-bound FT samples but was completely undetectable in co-IP'd protein samples (Fig. 2C). Thus the data indicates that despite strong P2X$_1$ pulldown, there is no P2X$_4$ and Nt5e associated with it.

We then performed the converse experiment with co-immunoprecipitation by anti-P2X$_4$ antibody (Fig. 3). As judged by Fig. 3B, P2X$_4$ protein (70 kD) was highly accumulated in IP fractions from wild type bladder but which disappeared in P2X$_4$ knockout samples. P2X$_1$ protein was highly concentrated in non-bound FT samples, but was detectable, albeit lightly in co-IP fractions (Fig. 3A). Given that the P2X$_4$ antibody is likely to have some cross-reactivity to P2X$_1$ the presence of weak bands in the IP fractions of Fig. 3A,B are to be expected. This muddies the interpretation somewhat, due to one imperfect antibody, however, if one accepts the high likelihood that anti-P2X$_4$ cross-reacts minimally with P2X$_1$, taken together data from these reverse IP experiments supports the conclusion that P2X$_1$ and P2X$_4$ do not form functional trimers. The overall optimization of conditions to ensure 'clean' pulldowns by bead-linked antibodies, is confirmed by Nt5e immunoblot in the P2X$_4$ pulldown experiment (Fig. 3C).
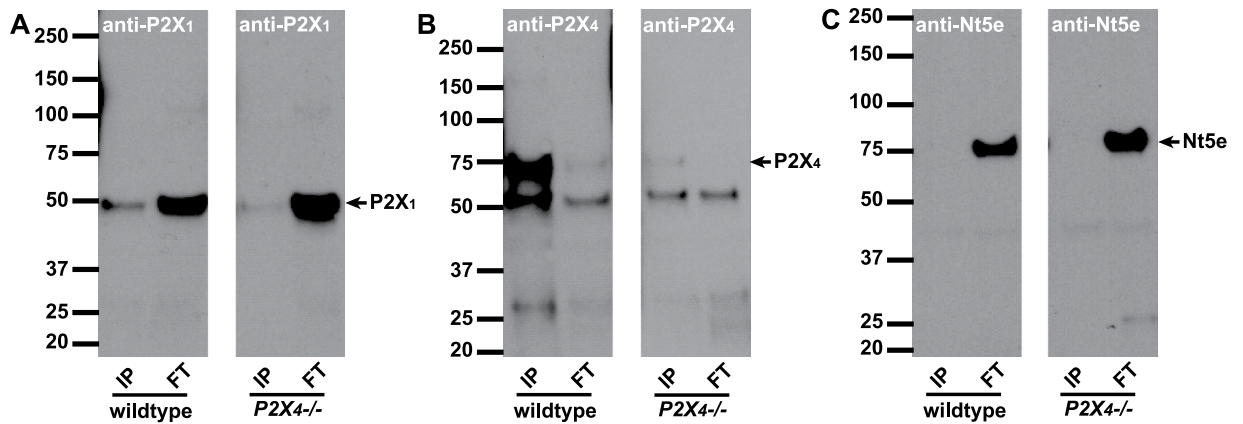
**Figure 3.** Immunoprecipitation with anti-P2X$_4$ antibody. Antibodies to P2X$_4$ were immobilized onto resin beads and then incubated with mouse bladder lysates to IP the antigen and co-IP interacting proteins. Proteins that were bound (IP: 2.5 μg protein/lane) or did not bind (FT: 25 μg protein/lane) to the beads, were resolved by SDS-PAGE, and Western blots were probed with **A**) P2X$_1$, B) P2X$_4$ or **C**) Nt5e antibodies. (**A**) Left and right panels show P2X$_1$ immunoblots on IP and FT lysates from wild type and *P2X$_4$ −/−* mice. P2X$_1$ is highly concentrated in the FT fractions. Minor potential P2X$_1$ staining appears in the IP lane, however this is due to P2X$_4$ antibody cross-reacting and pulling down some P2X$_1$. (**B**) P2X$_4$ antibody detects P2X$_4$ as a band at 70 kDa in wild type IP lane, but is absent in *P2X$_4$ −/−* mice. The antibody shows minor cross-reactivity to P2X$_1$ (50 kDa band). (**C**) An antibody to 5′-nucleotidase (Nt5e) demonstrates that pulldown with anti-P2X$_4$ is 'clean' with no non-specific protein binding evident in the IP lanes.

**P2X$_4$ is expressed in bladder, but not in the BSM.** P2X$_4$ was reported to be abundantly expressed in smooth muscle, including in BSM[22,31]. It was also reported that P2X$_1$ and P2X$_4$ can form functional heterotrimers in both native and artificial systems[25,31–34]. Our co-IP data did not support a P2X$_1$/P2X$_4$ heteromer in the bladder. Further support for this conclusion was provided by immunofluorescent staining and confocal imaging, which indicated that P2X$_4$ is expressed in the bladder wall but is not in smooth muscle itself (Fig. 4). The left panels (top) show discrete punctate P2X$_4$ staining in wild type bladder (white arrowheads) and these appear to be true P2X$_4$ positive cells because that unique staining pattern is absent in *P2X$_4$ −/−* bladders (left middle panel). There is however non-specific labelling of thin fibrous structures in the P2X4 knockout (white arrows).

Entpd2 (in red) is an ectonucleotidase that we have shown is specifically expressed in interstitial cells that tend to wrap around smooth muscle bundles in bladder[30]. From the merged panel it appears that P2X$_4$ positive cells are detected between muscle bundles and some are possibly associated with vascular elements. To our surprise, we were unable to detect a significant P2X$_4$ signal in BSM. However, BSM was strongly labelled by P2X$_1$ antibody (Fig. 4 bottom green), which is consistent with our Co-IP data and previous reports. In an attempt to reconcile our data with previous reports of strong P2X$_4$ staining[22,35] we used the same commercially available anti-P2X$_4$ antibody (Enzo Life Sciences: catalogue #: Alx-215-033-R100). Non-specific protein bands (western blot) and a strong immunofluorescent signal were detected in BSM of both wildtype and *P2X$_4$ −/−* mice using this antibody (Supplemental Figure 1), thus indicating that these earlier reports may have been misled as a result of poor antibodies.

To further define the non-specific immunostaining of thin fibers in the P2X$_4$ knockout we co-labeled cryosections with anti-PGP9.5, anti-β1 integrin, and anti- PDGFRα antibodies. Our results indicate that the fibrous structures do not co-localize with either β1 integrin signalling, which stains BSM strongly, or interstitial cell marker PDGFRα. They do however, co-label with nerve marker PGP.9.5, indicating those structures are very likely to be sensory nerve fibers, since P2X$_{2/3}$ has well documented expression there[36] (Supplemental Figure 2). In summary these data indicate that P2X$_4$ is expressed in bladder wall but not in BSM cells.

**Mice null for P2X$_4$ do not exhibit abnormal urinary function or abnormal BSM contractility.** *P2X$_4$ −/−* mice were further used to evaluate whether P2X$_4$ plays a role in regulating voiding function. Both male and female *P2X$_4$ −/−* mice have similar body weights to wild type mice. Their bladders are also visually normal with the weight in the normal range (Table 1). Voiding spot assay indicates that these mice have normal voiding volume, voiding spot numbers, and voiding spot size per void (Fig. 5).

We next performed cystometrograms on *P2X$_4$ −/−* mice (Fig. 6), and none of the analysed cystometric parameters showed any significant differences compared to wild type mice. These included voiding interval, basal pressure, micturition threshold pressure, peak pressure, and bladder compliance (Fig. 6C), thus confirming that *P2X$_4$ −/−* mice have undetectable changes of voiding function. Likewise, myography studies indicate that urothelium denuded BSM strips from *P2X$_4$ −/−* mice have normal contractility in response to EFS, including both the muscarinic and atropine resistant force components (Fig. 7). In summary, these data suggest that P2X$_4$ does not contribute to physiological voiding function in mice.
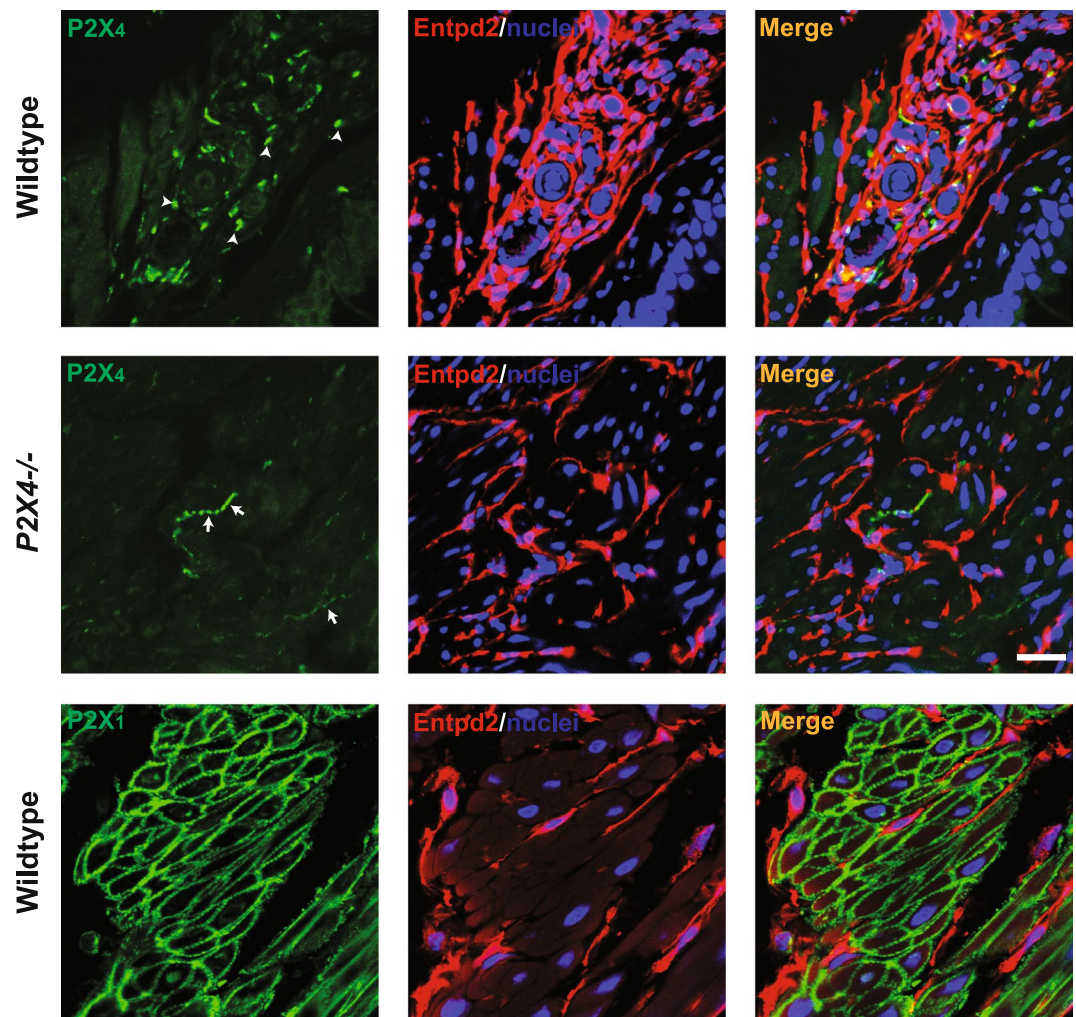
**Figure 4.** $P2X_4$ is expressed in bladder wall but not in BSM. Cryosections of mouse (wild type and $P2X_4-/-$) bladders were labelled with antibodies to $P2X_4$ (green), $P2X_1$ (green), ENTPD2 (red), and Topro-3 to label nuclei (blue). Entpd2 (middle panels) labels interstitial cells among muscle bundles. Colour merged panels are shown on the right and merged signals are seen as yellow. White arrowheads (top left) indicate $P2X_4$ labelling of unknown cellular structures. White arrows (middle left) indicate non-specific labelling by anti-$P2X_4$ antibody in $P2X_4-/-$ mice. $P2X_1$ receptors are abundantly expressed in BSM and that signal is clearly differentiated from interstitial cell staining (red). White scale bars = 10 μm.

| | Male | | Female | |
|---|---|---|---|---|
| | Wild type (n = 7) | $P2X_4-/-$ (n = 7) | Wild type (n = 8) | $P2X_4-/-$ (n = 6) |
| Body weight (g) | 26.83 ± 2.67 | 27.39 ± 2.51 | 20.75 ± 2.10 | 21.83 ± 1.88 |
| Bladder weight (mg) | 26.28 ± 2.41 | 27.11 ± 2.17 | 20.78 ± 1.74 | 21.20 ± 2.45 |
| Bladder/body ratio (mg/g) | 0.98 ± 0.08 | 0.99 ± 0.06 | 1.01 ± 0.04 | 0.97 ± 0.07 |

**Table 1.** $P2X_4-/-$ mice have normal body and bladder weights.

## Discussion

$P2X_4$ is reported to be expressed in many types of cells including glial cells in nerve tissue, vascular endothelial cells, macrophages, T lymphocytes, smooth muscle cells, and some epithelial cells[31]. In human vascular endothelial cells, $P2X_4$ channels mediate ATP-induced calcium influx in response to fluid shear stress[37–39]. This mechanism is crucial in regulating blood pressure and vascular remodelling, and mice null for $P2X_4$ exhibit higher blood pressure with reduced nitric oxide secretion[40]. $P2X_4$ is well recognized to be involved in both acute and chronic pain responses. Upon injury or inflammation, microglial $P2X_4$ is up-regulated, which mediates increased secretion of brain-derived neurotrophic factor (BDNF) and phosphorylation of Src family kinases Lyn, and these pathways are critical for neuropathic pain sensation[41–46]. Consistently, reduced pain responses and altered hippocampal synaptic potentiation have been observed in $P2X_4$ null mice[47,48].
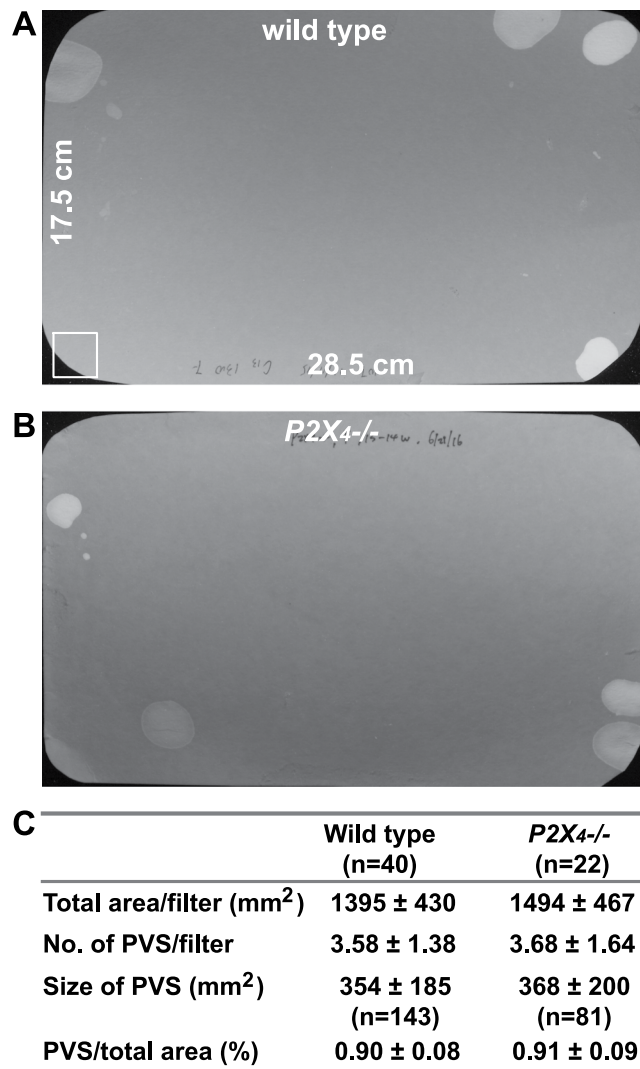
**Figure 5.** $P2X_4 -/-$ mice exhibit normal voiding behaviour by void spot assay. Representative filters showing urine spots under UV light from a wild type mouse (**A**) and a $P2X_4 -/-$ mouse (**B**). Quantitative data are shown in (**C**) and indicates $P2X_4 -/-$ mice have normal voiding volume, spot number, and spot size. The square at bottom left of panel (**A**) (surface area of $400\,mm^2$) serves as a size standard.

The presence of $P2X_4$ receptors in the bladder wall was noted long ago, and a quantitative analysis of transcripts indicated that it was the second most abundant P2X receptor (after $P2X_1$) in normal human bladder wall[15,16,18,22,49]. $P2X_4$ has been identified in BSM and lamina propria by immunolocalization, however, its functional role has not been studied yet. Interestingly, it has been observed that $P2X_4$ is significantly up-regulated in rabbit bladders upon ischemia and oxidative stress, and in the bladders of patients with symptomatic outlet obstruction, suggesting a potential role in the pathogenesis of bladder dysfunction[17,50].

In this study, we have confirmed that atropine resistant BSM contraction is insensitive to selective and potent $P2X_1$ antagonists NF279 and NF449, but seems partially sensitive to $P2X_4$ antagonist 5-BDBD (Fig. 1). This unique characterization of BSM has been noticed by several other studies, and a recent review article has provided a comprehensive summary[23]. Briefly, BSM atropine resistant force is partially $\alpha,\beta$-meATP sensitive, and P2X antagonists like reactive blue 2, PPADS, suramin, and $P2X_1$ selective antagonists NF279, NF449, MRS2159 are not very effective or even have no effect in inhibiting this atropine resistant force[23]. Interestingly, $P2X_4$ is a unique P2X member which is not inhibited by reactive blue 2, PPADS, or suramin[51], thus it was recently proposed that $P2X_1$ and $P2X_4$ might form heteromers in BSM[23]. Our pharmacological results are consistent with previous reports, and in combination with earlier morphological data showing strong P2X4 staining of BSM, led us to hypothesize that $P2X_4$ in the BSM might form a functional heteromer with the dominant $P2X_1$.

Functional heteromeric $P2X_1$ and $P2X_4$ receptors have been suggested in both artificial *Xenopus* oocytes expression system and native mouse macrophages and T lymphocytes[25,32–34]. This heteromeric channel is sensitive to $\alpha,\beta$-meATP and PPADS, but it is not very sensitive to suramin and can only be partially inhibited at high concentration. These pharmacological properties in other cellular systems resemble closely the BSM response to these drugs, supporting our hypothesis. To our surprise, the co-IP data clearly indicated that $P2X_1$ and $P2X_4$ do
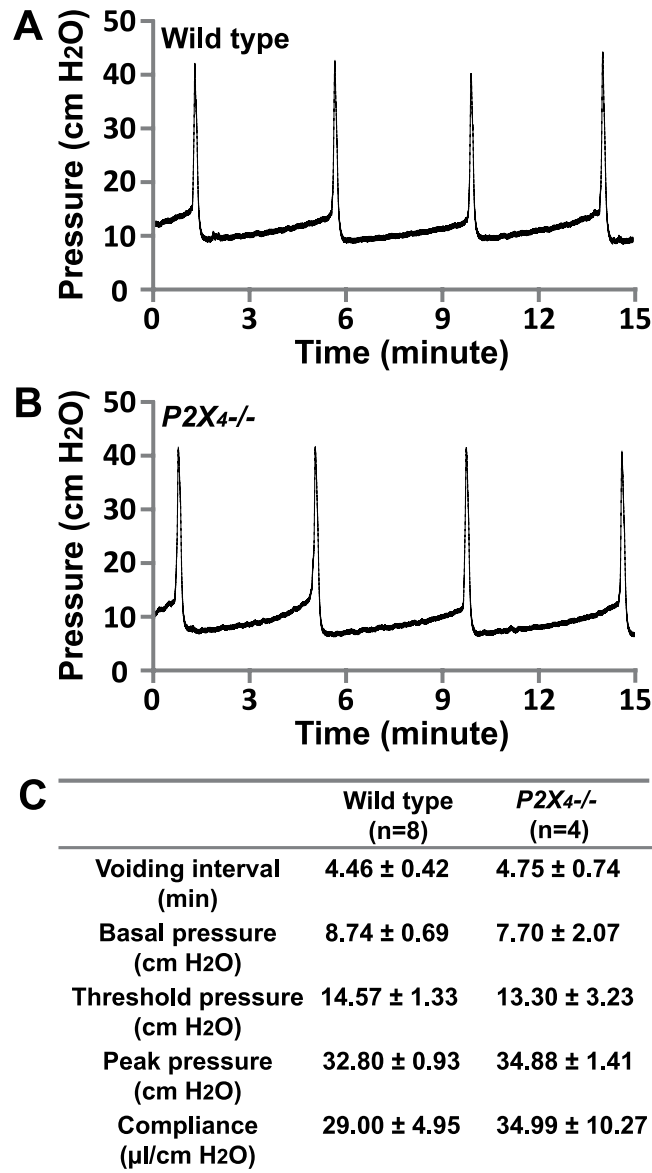
**Figure 6.** Cystometrograms showing intrabladder pressure throughout multiple filling/emptying cycles indicate that $P2X_4-/-$ mice have normal voiding interval, pressure, and bladder compliance; (**A**) CMG trace for a wild type mouse; (**B**) CMG trace for a $P2X_4-/-$ mouse; (**C**) Quantitation of cystometric parameters showing no significant differences between wild type and $P2X_4-/-$ mice.

not form heteromers in mouse bladder at all (Figs 2 and 3), and furthermore, our IF and imaging data indicate that P2X$_4$ is not present in BSM cells, but in a small unknown cellular structure that is dispersed within muscle bundles, and in particular associated with circular structures that might be vasculature (Fig. 4). We do not know the identity of this P2X$_4$ positive structure, but it could relate to neuronal structures, which are thought to have interactions with ENTPD2 positive interstitial cells located among muscle bundles[52]. It is possible that P2X$_1$ forms homomeric receptors in BSM as suggested by P2X$_1$ null mice, in which the BSM loses the majority of its purinergic force[14]. However, the potential existence of other P2X receptors, the non-typical P2X$_1$ pharmacological properties of BSM, and the atropine resistant and $\alpha,\beta$-meATP insensitive force remains unexplained and requires further investigation.

Although P2X$_4$ is not present in BSM, its presence in the bladder wall might indicate that it plays some other functional role in regulating voiding. To examine this, we carefully characterized the voiding phenotype of P2X$_4$ null mice in multiple complementary ways, and our results indicate that bladders are not macroscopically different, their voiding function appears completely normal according to voiding spot assay and cystometrogram data, and the BSM exhibits normal overall as well as purinergic contractility (Fig. 7). These data collectively indicate that P2X$_4$ might not be a functional receptor for bladder contractility. It remains possible that P2X$_4$ could play a role in the pathology of bladder diseases such as in bladder pain sensation, which remains a poorly understood area.
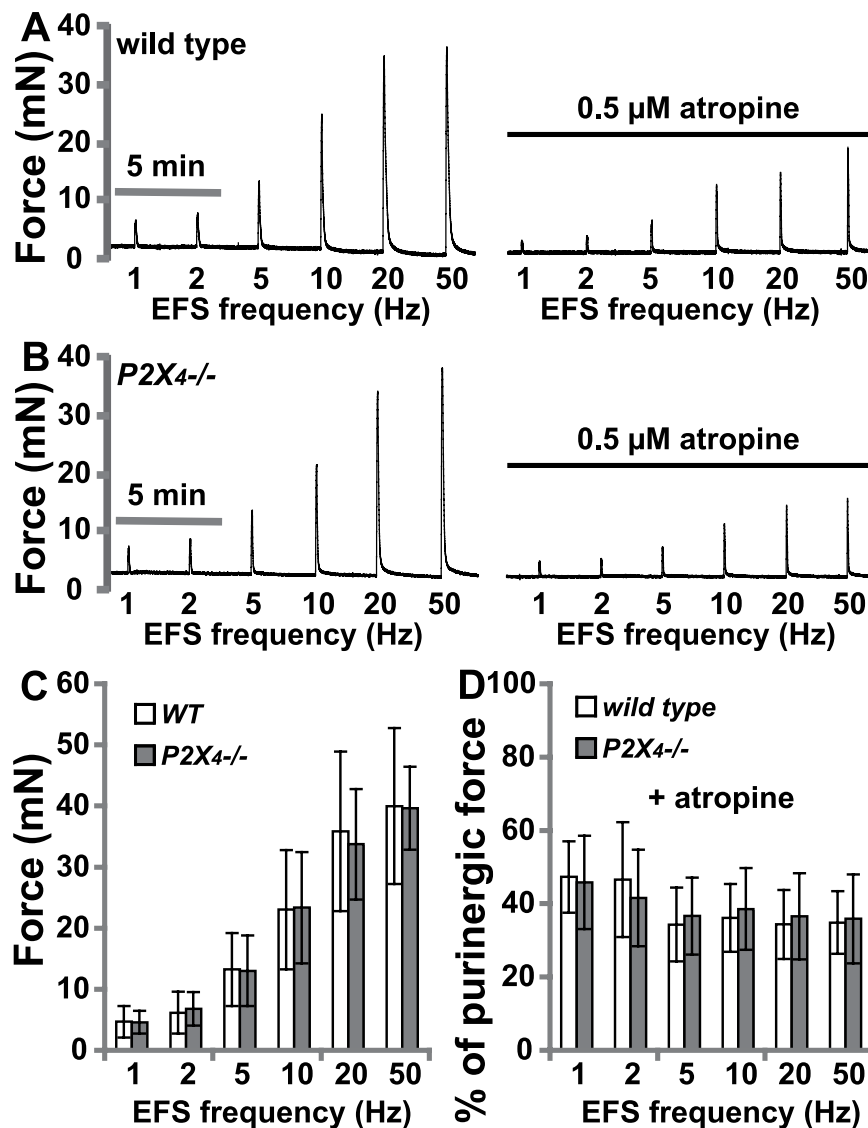
**Figure 7.** Myography indicates that BSM from $P2X_4-/-$ mice have normal contractility in response to electrical field stimulated neurotransmitter release. (**A**) Frequency train data on wild type bladder strips before and after atropine treatment; (**B**) Frequency train data on $P2X_4-/-$ bladder strips before and after atropine treatment; (**C**) and (**D**) Quantitation of force from wild type (n = 12) and $P2X_4-/-$ (n = 12) muscle strips. Data shown is mean ± SD.

## Materials and Methods

**Materials.** Unless otherwise specified, all chemicals were obtained from Sigma (St. Louis, MO) and were of reagent grade or better. Agonists and antagonists for P2X receptors were all purchased from R&D systems (Minneapolis, MN). All data generated or analyzed during this study are included in this published article.

**Animals.** Male and female C57BL/6 J mice (Jackson Laboratory, Bar Harbor, ME, USA) and $P2X_4-/-$ mice in C57BL/6 J background (kindly provided by Dr. Francois Rassendren, CNRS, France) (aged 12–16 weeks) were used in this study with the approval of the Beth Israel Deaconess Medical Centre Institutional Animal Care and Use Committee. Animals were used in adherence to NIH guidelines. All experiments and groups were performed under matching conditions for age and sex. Only male or female mice were used in some experiments (see below). If not specified, both male and female mice were used. Mice were euthanized by 100% $CO_2$ inhalation from a gas cylinder into a plexiglass chamber.

**Myography.** Bladders from male wild type and $P2X_4-/-$ mice were pinned on a small Sylgard block and bladder mucosa was dissected away carefully. BSM strips were then cut longitudinally (2–3 mm wide and 5–7 mm long) and mounted in an SI-MB4 tissue bath system (World Precision Instruments, FL, USA). Force sensors were connected to a TBM 4 M transbridge and the signal amplified by Powerlab and monitored through Chart software. Contraction force was monitored dynamically with a sampling rate of 2000/s. BSM strips were gently

pre-stretched to get optimized force and equilibrated for at least 1 h before any experiments. All experiments were conducted at 37 °C in physiological saline solution (PSS in mM: Na, 136.9; K, 5.9; Ca, 2.5; Mg, 1.2; Cl, 133.6; $HCO_3$, 15.5; $H_2PO_4$, 1.2; glucose, 11.5; pH 7.4), with continuous bubbling of 95% O2 and 5% CO2.

**Electrical field stimulation (EFS).**   EFS was carried out by a Grass S48 field stimulator (Grass Technologies, RI, USA) using standard protocols previously described[53].

**Co-Immunoprecipitation.**   Anti-$P2X_1$ (Catalogue #: APR-001, Alomone Labs) and anti-$P2X_4$ antibody (Catalogue #: APR-002, Alomone Labs) were pre-cleaned by Pierce Antibody Clean-up Kit (Thermo Fisher Scientific) for co-immunoprecipitation according to the manufacturer's instructions. Antibodies were then immobilized onto amine-reactive resin beads to IP the antigen and co-IP the interacting proteins using the Pierce Co-Immunoprecipitation (Co-IP) Kit (Thermo Fisher Scientific) to isolate protein complexes from native mouse bladder lysate according to the manufacturer. The isolated proteins were resolved on 8–16% polyacrylamide gradient gels under reducing condition (+0.1 M DTT and 95 °C for 5 min before loading), and further blotted and probed with anti-$P2X_1$, anti-$P2X_4$ and anti-5′-nucleotidase (NT5E) (Catalogue #: MAB44881, R&D system) antibodies for protein detection. If $P2X_1$ and $P2X_4$ form heteromers, pull-down of $P2X_1$ protein by $P2X_1$ antibody will also pull-down $P2X_4$, and vice versa.

**Western Blot.**   Excised whole bladders were put in 0.5 ml ice-cold radio immunoprecipitation assay buffer (RIPA; 50 mM Tris pH 8.0, 150 mM NaCl, 1% v/v NP-40, 0.5% w/v deoxycholic acid, 0.1% w/v SDS) containing Complete Mini Protease Inhibitor Cocktail tablets (Roche, Germany). Proteins were resolved by SDS-PAGE (Tris-HEPES 8–16% gel, catalogue #: NH11-816; NuSep, GA) in Tris-HEPES running buffer (12.1 g Tris, 23.8 g HEPES, 1.0 g SDS, and $H_2O$ to 1000 ml) at 120 constant voltage for 45–60 min, and then transferred to Immun-Blot PVDF membrane (BioRad Laboratories, Hercules, CA) in transfer buffer (Tris base 3.0 g, bicine 4.08 g, methanol 100 ml, and $H_2O$ to 1000 ml) at 350 mA for 90-120 min at 4 °C. The blots were blocked in 5% dehydrated milk in PBS overnight at 4 °C, and then were probed with specific antibodies in 1% dehydrated milk in PBS for 2 hours at room temperature, followed by the appropriate species-specific secondary antibodies conjugated to HRP for 1 hour at room temperature. Three time 15 min washes were performed after the first and the secondary antibodies incubation with TBS Tween 20 (0.05%). Bands were detected using ECL Plus Western Blotting reagents (GE Healthcare, Piscataway, NJ) and CL-X Posure film (Thermo Scientific, Rockford, Il). The film was developed, scanned and images were imported into Adobe Illustrator CS3 (San Jose, CA).

**Immunofluorescence (IF) staining and confocal microscopy.**   Both wild type and $P2X_4−/−$ mice were sacrificed for IF staining as previously described[54]. Excised bladders were fixed in 4% (wt/vol) paraformaldehyde for 2 hours at room temperature. Fixed tissue was cryoprotected, frozen, sectioned, and incubated with rabbit polyclonal anti-$P2X_4$ antibody (Catalogue #: APR002, Alomone lab), polyclonal sheep anti-ENTPD2 antibody (Catalogue #: AF5797, R&D systems, Minneapolis, MN), monoclonal PDGFRα affinity purified goat IgG antibody (Catalogue #: AF1062, R&D system, Minneapolis, MN), chicken polyclonal anti-PGP9.5 antibody (Catalogue #: ab72910, ABCAM, Cambridge, MA), and purified rat anti-mouse β1 integrin antibody (Catalogue #: 550531, BD Bioscience, San Jose, CA) (1:100 dilution) overnight at 4 °C. The sections were then incubated with a mixture of Alexa 488-conjugated secondary antibody (diluted 1:100), Alex 546-conjugated secondary antibody (diluted 1:100), and Topro-3 (1:1,000). Imaging was performed on a Zeiss LSM-510 confocal microscope equipped with argon and green and red helium-neon lasers (Thornwood, NY). Images were acquired by sequential scanning with a 63X (1.4 numerical aperture) planapochromat oil objective. The images (512 & 512 pixels) were saved as TIFF files, and were imported into Adobe Illustrator CS3. In the current study, each bladder was sectioned to obtain 2 slides with 4–5 sections of tissue on each slide. Each tissue section was examined under the microscope to ensure the consistency of the staining result, and representative images were taken.

**Spontaneous voiding spot assay (VSA).**   VSA's were performed as described previously[55,56]. Male mice can exhibit dominant and territorial marking behaviour, therefore only female mice were used in this experiment. Individual mice were gently placed in a standard polycarbonate mouse cage with Blicks Cosmos Blotting Paper (Cat #10422-1005) placed in the bottom, for 4 hours. Mice were given standard dry mouse chow for the duration of the assay. Water was withheld due to problems created by water dripping onto the filter paper. After 4 hours mice were returned to their home cages and the filter paper was allowed to dry. Filters were photographed under ultraviolet light at 365 nm in a UVP Chromato-Vue C-75 system (UVP, Upland, CA) that incorporates an onboard Canon digital single lens reflex camera (EOS Rebel T3 – 12 megapixels). Overlapping voiding spots were visually examined and manually separated by outlining and copying, then pasting to a nearby empty space in ImageJ software (http://fiji.sc/wiki/index.php/Fiji). Images were analyzed by UrineQuant software developed by us in collaboration with the Harvard Imaging and Data Core. The results table, which contains the area of each voiding spot and total number of spots, were imported into Excel software for further statistical processing. A volume:area standard curve on this paper determined that $1 mm^2$ is equal to 0.283 μl of urine. Voiding spots that have an area $\geq 80 mm^2$ are considered to be primary voiding spots (PVS)[55].

**Cystometrograms (CMG).**   CMG was performed as described previously and only female mice were used in this experiment.[55,56]. Mice were anesthetized by subcutaneous injection of urethane (1.4 g/kg). Once the pedal reflex was absent, a 1 cm midline abdominal incision was performed and a flame flanged PE50 tubing was implanted through the dome of the bladder, which was secured in place with an 8–0 silk surgical suture. The mouse was placed into a restrainer and the catheter was connected to a pressure transducer (and syringe pump by side arm) coupled to data acquisition devices (WPI Transbridge [Sarasota, FL] and AD Instruments Powerlab 4/35 [Colorado Springs CO]) and computerized recording system (AD Instruments LabChart software).

**Statistical analyses.** Data are presented as mean ± standard deviation (SD). Data were analysed using Student's *t*-test for paired groups or one-way analysis of variance (ANOVA) for comparison among groups. Bonferroni's multiple comparison post-hoc tests were used where necessary and P < 0.05 was considered to be significant.

## References

1. Coyne, K. S. *et al.* The prevalence of lower urinary tract symptoms (LUTS) in the USA, the UK and Sweden: results from the Epidemiology of LUTS (EpiLUTS) study. *BJU Int* **104**, 352–360 (2009).
2. Irwin, D. E., Kopp, Z. S., Agatep, B., Milsom, I. & Abrams, P. Worldwide prevalence estimates of lower urinary tract symptoms, overactive bladder, urinary incontinence and bladder outlet obstruction. *BJU Int* **108**, 1132–1138 (2011).
3. Cowan, W. D. & Daniel, E. E. Human female bladder and its noncholinergic contractile function. *Can J Physiol Pharmacol* **61**, 1236–1246 (1983).
4. Speakman, M. J., Walmsley, D. & Brading, A. F. An *in vitro* pharmacological study of the human trigone–a site of non-adrenergic, non-cholinergic neurotransmission. *Br J Urol* **61**, 304–309 (1988).
5. Burnstock, G. Purinergic signaling in lower urinary tract. *Handbook of experimental pharmacology* **151**, 423–515 (2001).
6. Palea, S. *et al.* ADP beta S induces contraction of the human isolated urinary bladder through a purinoceptor subtype different from P2X and P2Y. *J Pharmacol Exp Ther* **269**, 193–197 (1994).
7. Andersson, K. E. & Arner, A. Urinary bladder contraction and relaxation: physiology and pathophysiology. *Physiol Rev* **84**, 935–986 (2004).
8. Boselli, C., Govoni, S., Condino, A. M. & D'Agostino, G. Bladder instability: a re-appraisal of classical experimental approaches and development of new therapeutic strategies. *J Auton Pharmacol* **21**, 219–229 (2001).
9. Ouslander, J. G. Management of overactive bladder. *N Engl J Med* **350**, 786–799 (2004).
10. Palea, S., Artibani, W., Ostardo, E., Trist, D. G. & Pietra, C. Evidence for purinergic neurotransmission in human urinary bladder affected by interstitial cystitis. *J Urol* **150**, 2007–2012 (1993).
11. Saito, M., Kondo, A., Kato, T., Hasegawa, S. & Miyake, K. Response of the human neurogenic bladder to KCl, carbachol, ATP and CaCl2. *Br J Urol* **72**, 298–302 (1993).
12. Sjogren, C., Andersson, K. E., Husted, S., Mattiasson, A. & Moller-Madsen, B. Atropine resistance of transmurally stimulated isolated human bladder muscle. *J Urol* **128**, 1368–1371 (1982).
13. Nardi-Schreiber, A. *et al.* Defective ATP breakdown activity related to an ENTPD1 gene mutation demonstrated using 31P NMR spectroscopy. *Chem Commun (Camb)* **53**, 9121–9124 (2017).
14. Heppner, T. J. *et al.* Nerve-evoked purinergic signalling suppresses action potentials, Ca2+ flashes and contractility evoked by muscarinic receptor activation in mouse urinary bladder smooth muscle. *J Physiol* **587**, 5275–5288 (2009).
15. Creed, K. E., Loxley, R. A. & Phillips, J. K. Functional expression of muscarinic and purinoceptors in the urinary bladder of male and female rats and guinea pigs. *J Smooth Muscle Res* **46**, 201–215 (2010).
16. Lee, H. Y., Bardini, M. & Burnstock, G. Distribution of P2X receptors in the urinary bladder and the ureter of the rat. *J Urol* **163**, 2002–2007 (2000).
17. O'Reilly, B. A. *et al.* A quantitative analysis of purinoceptor expression in the bladders of patients with symptomatic outlet obstruction. *BJU Int* **87**, 617–622 (2001).
18. Vial, C. & Evans, R. J. P2X receptor expression in mouse urinary bladder and the requirement of P2X(1) receptors for functional P2X receptor responses in the mouse urinary bladder smooth muscle. *Br J Pharmacol* **131**, 1489–1495 (2000).
19. Kennedy, C., Tasker, P. N., Gallacher, G. & Westfall, T. D. Identification of atropine- and P2X1 receptor antagonist-resistant, neurogenic contractions of the urinary bladder. *J Neurosci* **27**, 845–851 (2007).
20. Kendig, D. M., Ets, H. K. & Moreland, R. S. Effect of type II diabetes on male rat bladder contractility. *Am J Physiol Renal Physiol* **310**, F909–922 (2016).
21. Liu, G. & Daneshgari, F. Alterations in neurogenically mediated contractile responses of urinary bladder in rats with diabetes. *Am J Physiol Renal Physiol* **288**, F1220–1226 (2005).
22. Bo, X. *et al.* Tissue distribution of P2X4 receptors studied with an ectodomain antibody. *Cell Tissue Res* **313**, 159–165 (2003).
23. Kennedy, C. ATP as a cotransmitter in the autonomic nervous system. *Auton Neurosci* **191**, 2–15 (2015).
24. Kugelgen, I. v. Pharmacology of mammalian P2X- and P2Y-receptors. *Biotrend* **3** (2008).
25. Roberts, J. A. *et al.* Molecular properties of P2X receptors. *Pflugers Arch* **452**, 486–500 (2006).
26. Weisman, G. A., Woods, L. T., Erb, L. & Seye, C. I. P2Y receptors in the mammalian nervous system: pharmacology, ligands and therapeutic potential. *CNS Neurol Disord Drug Targets* **11**, 722–738 (2012).
27. Ashour, F., Atterbury-Thomas, M., Deuchars, J. & Evans, R. J. An evaluation of antibody detection of the P2X1 receptor subunit in the CNS of wild type and P2X1-knockout mice. *Neurosci Lett* **397**, 120–125 (2006).
28. Mulryan, K. *et al.* Reduced vas deferens contraction and male infertility in mice lacking P2X1 receptors. *Nature* **403**, 86–89 (2000).
29. Wyatt, L. R. *et al.* Contribution of P2X4 receptors to ethanol intake in male C57BL/6 mice. *Neurochem Res* **39**, 1127–1139 (2014).
30. Yu, W., Robson, S. C. & Hill, W. G. Expression and distribution of ectonucleotidases in mouse urinary bladder. *PLoS One* **6**, e18704 (2011).
31. Saul, A., Hausmann, R., Kless, A. & Nicke, A. Heteromeric assembly of P2X subunits. *Front Cell Neurosci* **7**, 250 (2013).
32. Nicke, A., Kerschensteiner, D. & Soto, F. Biochemical and functional evidence for heteromeric assembly of P2X1 and P2X4 subunits. *J Neurochem* **92**, 925–933 (2005).
33. Sim, J. A., Park, C. K., Oh, S. B., Evans, R. J. & North, R. A. P2X1 and P2X4 receptor currents in mouse macrophages. *Br J Pharmacol* **152**, 1283–1290 (2007).
34. Woehrle, T. *et al.* Pannexin-1 hemichannel-mediated ATP release together with P2X1 and P2X4 receptors regulate T-cell activation at the immune synapse. *Blood* **116**, 3475–3484 (2010).
35. Moller, S. *et al.* Monitoring the expression of purinoceptors and nucleotide-metabolizing ecto-enzymes with antibodies directed against proteins in native conformation. *Purinergic Signal* **3**, 359–366 (2007).
36. Cockayne, D. A. *et al.* P2X2 knockout mice and P2X2/P2X3 double knockout mice reveal a role for the P2X2 receptor subunit in mediating multiple sensory effects of ATP. *J Physiol* **567**, 621–639 (2005).
37. Schwiebert, L. M., Rice, W. C., Kudlow, B. A., Taylor, A. L. & Schwiebert, E. M. Extracellular ATP signaling and P2X nucleotide receptors in monolayers of primary human vascular endothelial cells. *Am J Physiol Cell Physiol* **282**, C289–301 (2002).
38. Yamamoto, K., Korenaga, R., Kamiya, A. & Ando, J. Fluid shear stress activates Ca(2+) influx into human endothelial cells via P2X4 purinoceptors. *Circ Res* **87**, 385–391 (2000).
39. Yamamoto, K. *et al.* P2X(4) receptors mediate ATP-induced calcium influx in human vascular endothelial cells. *Am J Physiol Heart Circ Physiol* **279**, H285–292 (2000).
40. Yamamoto, K. *et al.* Impaired flow-dependent control of vascular tone and remodeling in P2X4-deficient mice. *Nat Med* **12**, 133–137 (2006).
41. Cheng, R. D., Ren, J. J., Zhang, Y. Y. & Ye, X. M. P2X4 receptors expressed on microglial cells in post-ischemic inflammation of brain ischemic injury. *Neurochem Int* **67**, 9–13 (2014).
42. Inoue, K. & Tsuda, M. P2X4 receptors of microglia in neuropathic pain. *CNS Neurol Disord Drug Targets* **11**, 699–704 (2012).

43. Trang, T. & Salter, M. W. P2X4 purinoceptor signaling in chronic pain. *Purinergic Signal* **8**, 621–628 (2012).
44. Tsuda, M., Masuda, T., Tozaki-Saitoh, H. & Inoue, K. P2X4 receptors and neuropathic pain. *Front Cell Neurosci* **7**, 191 (2013).
45. Tsuda, M. *et al*. Lyn tyrosine kinase is required for P2X(4) receptor upregulation and neuropathic pain after peripheral nerve injury. *Glia* **56**, 50–58 (2008).
46. Ulmann, L. *et al*. Up-regulation of P2X4 receptors in spinal microglia after peripheral nerve injury mediates BDNF release and neuropathic pain. *J Neurosci* **28**, 11263–11268 (2008).
47. Sim, J. A. *et al*. Altered hippocampal synaptic potentiation in P2X4 knock-out mice. *J Neurosci* **26**, 9006–9009 (2006).
48. Tsuda, M. *et al*. Behavioral phenotypes of mice lacking purinergic P2X4 receptors in acute and chronic pain assays. *Mol Pain* **5**, 28 (2009).
49. O'Reilly, B. A. *et al*. A quantitative analysis of purinoceptor expression in human fetal and adult bladders. *J Urol* **165**, 1730–1734 (2001).
50. Zhang, Q., Siroky, M., Yang, J. H., Zhao, Z. & Azadzoi, K. Effects of ischemia and oxidative stress on bladder purinoceptors expression. *Urology* **84**(1249), e1241–1247 (2014).
51. Bo, X., Zhang, Y., Nassar, M., Burnstock, G. & Schoepfer, R. A P2X purinoceptor cDNA conferring a novel pharmacological profile. *FEBS Lett* **375**, 129–133 (1995).
52. Yu, W., Zeidel, M. L. & Hill, W. G. Cellular expression profile for interstitial cells of cajal in bladder - a cell often misidentified as myocyte or myofibroblast. *PLoS One* **7**, e48897 (2012).
53. Sibley, G. N. A comparison of spontaneous and nerve-mediated activity in bladder muscle from man, pig and rabbit. *J Physiol* **354**, 431–443 (1984).
54. Yu, W., Hill, W. G., Apodaca, G. & Zeidel, M. L. Expression and distribution of transient receptor potential (TRP) channels in bladder epithelium. *Am J Physiol Renal Physiol* **300**, F49–59 (2011).
55. Rajandram, R. *et al*. Intact urothelial barrier function in a mouse model of ketamine-induced voiding dysfunction. *Am J Physiol Renal Physiol* **310**, F885–894 (2016).
56. Yu, W. *et al*. Spontaneous voiding by mice reveals strain-specific lower urinary tract function to be a quantitative genetic trait. *Am J Physiol Renal Physiol* **306**, F1296–1307 (2014).

## Acknowledgements

## Author Contributions

W.Y. conceived and designed the experiments. W.Y. performed the research, collected and analyzed data. W.Y., W.H., S.R., and Z.M. contributed reagents/materials/analysis tools, and interpreted data. W.Y., W.H., S.R., and Z.M. wrote the paper. All authors read and approved the final manuscript.

## Additional Information

**Supplementary information** accompanies this paper at https://doi.org/10.1038/s41598-018-20216-4.

**Competing Interests:** The authors declare that they have no competing interests.

**Publisher's note:** Springer Nature remains neutral with regard to jurisdictional claims in published maps and institutional affiliations.